AERO-THERMAL DESIGN AND TESTING OF ADVANCED TURBINE BLADES

M. Haendler, D. Raake, M. Scheurlen
Siemens AG
Power Generation (KWU)
Muelheim a. d. Ruhr, Germany

ABSTRACT

Based on the experience gained with more than 80 machines operating worldwide in 50 and 60 Hz electrical systems respectively, Siemens has developed a new generation of advanced gas turbines which yield substantially improved performance at a higher output level. This "3A-Series" comprises three gas turbine models ranging from 70 MW to 240 MW for 50 Hz and 60 Hz power generation applications.

The first of the new advanced gas turbines with 170 MW and 3600 rpm was tested in the Berlin factory test facility under the full range of operation conditions. It was equipped with various measurement systems to monitor pressures, gas and metal temperatures, clearences, strains, vibrations and exhaust emissions.

This paper presents the aero-thermal design procedure of the highly thermal loaded film cooled first stage blading. The predictions are compared with the extensive optical pyrometer measurements taken at the Siemens test facility on the V84.3A machine under full load conditions. The pyrometer was inserted at several locations in the turbine and radially moved giving a complete surface temperature information of the first stage vanes and blades.

INTRODUCTION

Superior advantages of gas turbines can only be achieved if all its components are optimized with respect to the same target. For heavy duty gas turbines, which are applied predominantly in combined cycle power stations, this target is maximum combined cycle efficiency. The main parameter, which drives this efficiency, is the turbine inlet temperature according to the ISO 2314 standard. It can be interpreted as the fictitious mixing temperature of combustion gases with cooling air prior to turbine expansion. Thus, it is optimized by maximizing the firing temperature and, simultaneously, by minimizing the cooling air consumption for turbine blades. The second parameter is aerodynamic efficiency along the whole flow path, starting from the air intake, the compressor and its diffuser, combustor, turbine and finally the exhaust diffuser. The third parameter for optimizing the combined cycle efficiency is the pressure ratio of the gas turbine. The advanced model V84.3A combines all of these improvements.

ENGINE DESCRIPTION

A cross section of the new model V84.3A gas turbine is shown in Fig. 1. The basic design including the disk-type rotor, twin outboard bearing shaft support, cold-end generator drive and the axial exhaust diffuser has been adopted from previous Siemens gas turbines models. A major new design feature is the annular combustion system. A total of 24 uniformly spaced hybrid burners are arranged in a so-called Hybrid-Burner Ring (HBR) ahead of the spacious annular combustion chamber. Details of these machines has already been described by Becker et al. (1995).

The concept of the four-stage turbine was carried over from the previous-generation machine, but the "3A-Series" engine makes use of a more sophisticated cooling technique and improved blade materials and coatings. With the exception of the last stage blade, all vanes and blades are air cooled. Cooling air is provided at different pressure and temperature levels from compressor extractions to provide the best possible cooling effect and at the same time provide optimal unit thermal performance (Reichert and Janssen, 1996).

Free standing blades are utilized in all four stages. The front stage blades are unshrouded for durability considerations and the rear stage blades for performance reasons. Unshrouded rear stage blades permit a larger annulus area at a constant acceptable stress

Presented at the International Gas Turbine & Aeroengine Congress & Exhibition
Orlando, Florida — June 2–5, 1997

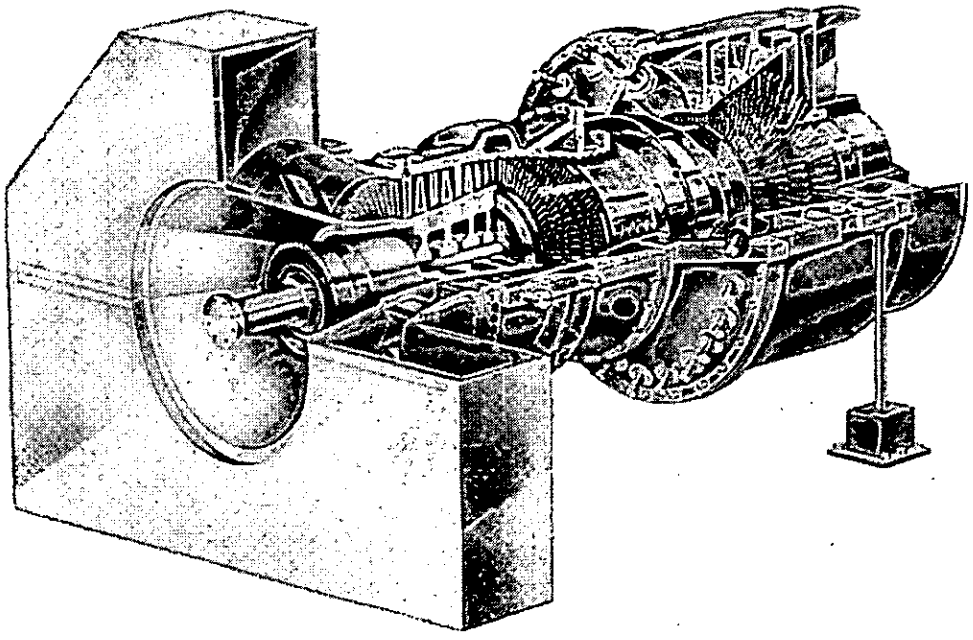

Fig. 1 V84.3A gas turbine

level thereby lowering Mach number levels for the airfoil. In addition, without shroud stress limitations, the number of blades can be reduced thereby achieving more optimal airfoil loadings (Schulenberg and Zimmermann, 1995).

Simple cycle performance data of the "3A-Series" gas turbines is listed in Table 1. The turbine sizes of the 50 Hz V94.3A and the 50/60 Hz V64.3A are scaled from the 60 Hz model V84.3A.

Table 1 "3A-Series" Gas Turbine Performance Data

Gas Turbine		V64.3A	V84.3A	V94.3A
Frequency	Hz	50 or 60	60	50
Speed	RPM	5400	3600	3000
Rating	MW	70	170	240
Efficiency	%	36.8	38.0	38.0

AERDDYNAMIC DESIGN

The aerodynamic design of the advanced turbine, which is based on a collaboration between Pratt & Whitney and Siemens Power Generation (Janssen et al., 1995), followed the standard design process shown in Fig. 2 (Casey, 1994). The airfoil design process itself started with the construction of an airfoil from spanwise sections which were developed on a quasi three-dimensional basis. An axisymmetric throughflow (S2m) calculation was used to define the mean hub-to-tip flow and several blade-to-blade (S1) computations to specify the Mach number distribution and the boundary layer development on the profile.

Airfoil pressure distributions from this computation were subsequently evaluated in terms of established criteria for acceptability and if found unacceptable the airfoils and/or flowpath were appropriately modified and the flow analysis repeated. Acceptibility of the predicted pressure distribution was judged based on the results of boundary layer computations and pressure distribution related criteria. This criteria take the form of parameters which have been calibrated from a very wide range of rig and engine data.

Figure 3 shows the pressure distribution along pressure and suction side of the first stage vane mean section. In this figure, 3D

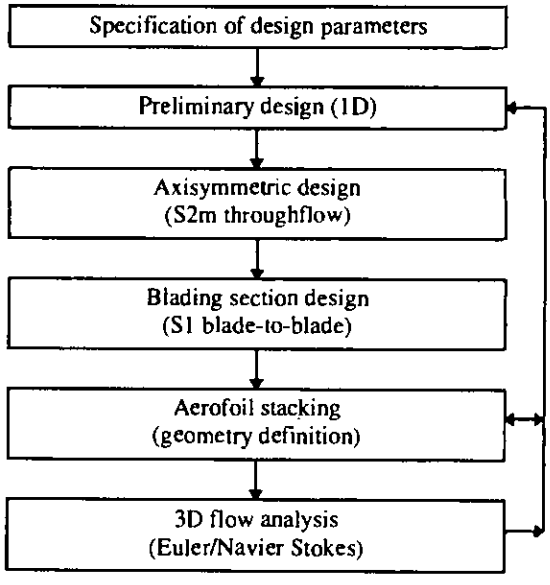

Fig. 2 Typical turbomachinery aerodynamic design system

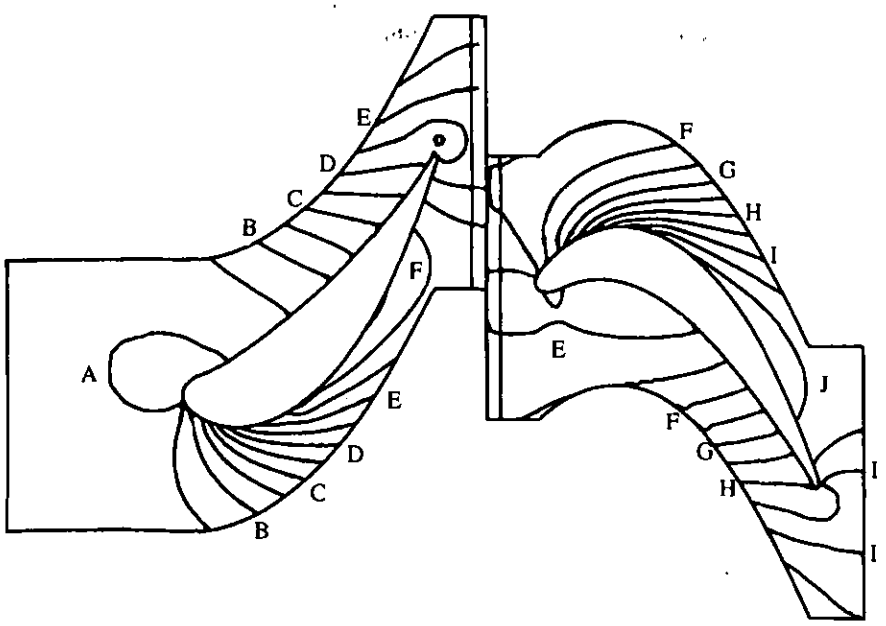

isoline	p/p_ref
A	1.00
B	0.95
C	0.90
D	0.85
E	0.80
F	0.75
G	0.70
H	0.65
I	0.60
J	0.55

Fig. 4 Predicted isolines of static pressure of the first stage vane and blade

Navier Stokes calculations with and without film cooling are compared. On the pressure side, the influence of the cooling air blowing is very little but on the suction side the local effect is evident.

To take the important interactions between adjacent blade rows into account, a 3D Navier Stokes flow computation of the whole stage follows the Q3D design. The code used was the commercial software package TASCflow. The turbulence effects are modelled using a modification of the standard k-ε turbulence model (Launder and Spalding, 1974) by Kato and Launder (1993). Figure 4 shows the isolines of static pressure of the first stage vane and blade mean section. In this calculation both stationary and rotating components are analyzed using a mixing plane approach at the sliding interface. The change in overall pressure ratio on the vane is due to the film mass addition.

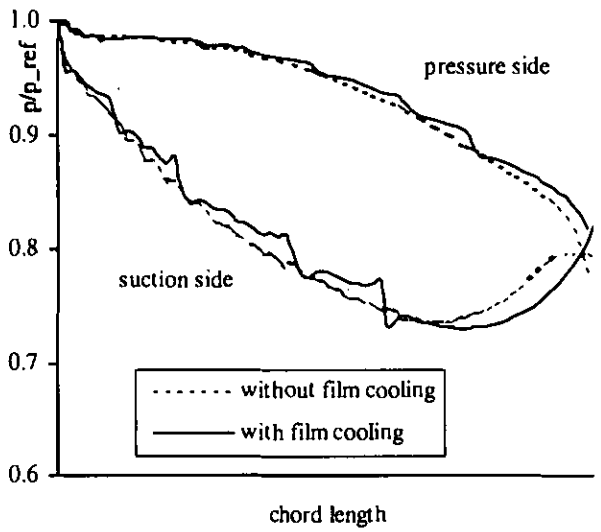

Fig. 3 Comparison of numerically predicted pressure distribution with and without film cooling

THERMAL DESIGN

The design requirement of the cooling system is based on the maximal allowable metal temperature with minimum cooling flow. The cooling system design of the highly loaded vanes and blades of the first turbine stage (firing temperature up to 1640K) followed an integrated process between the definition of the internal flow path, the calculation of external and internal heat transfer including pressure losses and the thermal analysis.

Cooling Scheme

The cooling schemes employed for the airfoils reflect the technology developed for high temperature aero-engines. The first vane which is cast from a cobalt alloy is shown in Fig. 5, the first stage blade is cast from a hot corrosion resistant single crystal alloy and is shown in Fig. 6.

The first vane features a two cavity design and a combination of impingement cooling, convection cooling and film cooling. The front cavity receives cooling air from its inner shroud. The rear vane section, which operates at a reduced main flow pressure level,

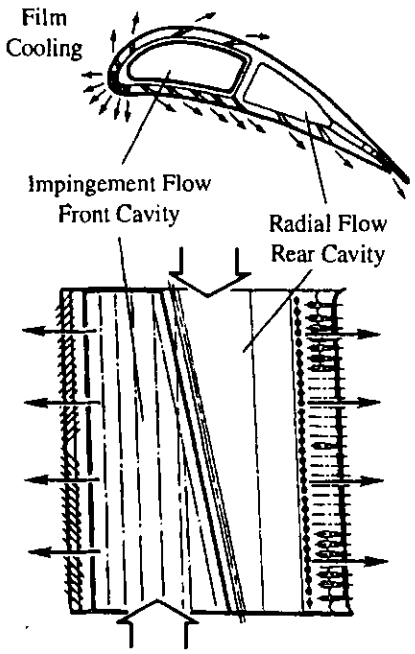

Fig. 5 Cooling scheme first stage vane

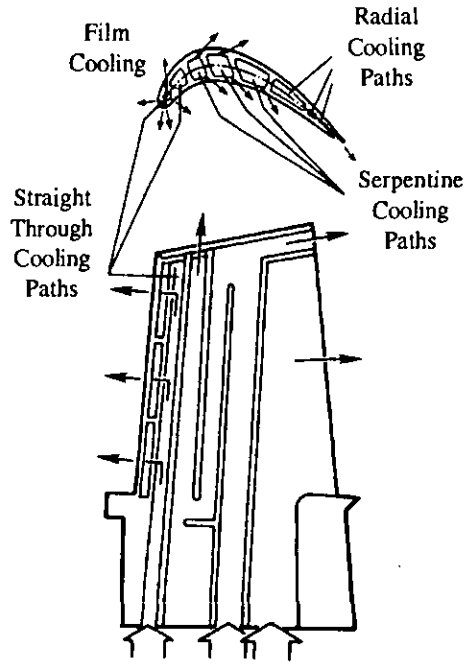

Fig. 6 Cooling scheme first stage blade

receives cooling air at its outer shroud. Flow in the front cavity enters by way of an insert which impinges the air onto the inner surfaces to achieve enhanced internal heat transfer. The air is then discharged to the main gas flow path through film holes in the leading edge and on the pressure and suction side. To increase the cooling efficiency, the film holes in the leading edge are inclined in radial direction and on pressure and suction side the hole exits are formed as so-called shaped holes. The rear cavity employs surface turbulator enhanced convective internal cooling. Flow from this cavity is discharged to the mainstream through pressure side film holes and out of the trailing edge. Trailing edge cooling flow discharge features a pressure side cutback scheme which achieves design metal temperatures with minimum airfoil blockage.

Inner and outer platforms of the first stage vane are also cooled by a combination of impingement, convective and film cooling. The cooling air discharged to the mainstream through film holes along the platform edges. In addition, a thermal barrier coating is utilized on the flowpath surfaces of the endwalls to reduce the effective heat load, thereby reducing cooling air requirements.

The cooling of the first rotating blade is achieved by a system of three independent working cooling channels. The first channel feeds cooling air through crossover holes into three radially separated cavities. From these cavities the air is discharged by cylindrical and radially inclined shower head holes cooling down the very leading edge of the blade. In addition, a row of shaped holes is pulling air from the cavities and is building up a cooling air film on the suction side. The use of the crossover holes has the advantage of increasing the internal heat transfer at the thermal highly loaded leading edge and, additionally, this design increases the fail safety of the blade in case of damage. The second channel in the middle of the blade builds up a multi pass system. Air is discharged from this channel by rows of shaped holes at the pressure and the suction side which are optimized to give a high film cooling effectiveness. The third channel supplies cooling air for the trailing edge of the blade and is similar designed like the first vane with a pressure side cut back scheme.

External and Internal Heat Transfer

The heat transfer coefficient (HTC) on the hot gas side has been calculated by a boundary layer code based on Scheuerer (1983) including the effects of free stream turbulence, wall roughness and surface curvature. At the leading edge a circular cylinder heat transfer model was used. The decrease of the hot gas temperature due to the film cooling has been taken into consideration in form of the film effectiveness calculated with L'Ecuyer and Soechting (1985), Kruse (1985) or Schoenung and Rodi (1987).

For the internal heat transfer analysis a Siemens code is used solving the one dimensional compressible flow equations for network systems with and without rotation. The necessary information for the heat transfer and friction coefficients are drawn from correlations.

The heat conduction problem in the thermal design procedure is solved in several two dimensional cuts of a blade by use of the commercial finite element code named COSMOS/M.

TEMPERATURE MEASUREMENTS

The gas turbine test facility was installed in the Berlin gas turbine manufacturing plant. It has the unique capability of testing gas turbine prototypes at any operational mode up to full load and off frequency conditions, thanks to the 170 MW water break to dissipate the mechanical output of the test machine.

Uses of infrared thermometry

Infrared thermometry is a proven technology for non-intrusive measurements of surface temperatures in gas turbine enviroments as described in the early years of application of this technique in gas turbine e.g. by Atkinson and Guenard (1978), Douglas (1980), Benyon (1981) and in the last years by Schulenberg and Bals (1987), Sellers et al. (1989) and Boehm et al. (1996). Research and development on the application of this measurement technique to gas turbines was reported in the past e.g. by Barber (1969), Rohy and Compton (1973), and in the recent past by Schenk et al. (1994), Moon et al. (1995) and Schenk and Raake (1996). The principal focus of research work on the use of infrared thermometry in gas turbines in the recent years was the development of computer models for the application and evaluation of this technique e.g. by De Lucia and Lanfranchi (1992) and De Lucia and Masotti (1995).

Siemens has been using turbine pyrometry for more than a decade in developing gas-turbine blade and vane cooling technology including the investigation of various designs and of the effects of manufacturing techniques.

Experimental setup

The investigations are carried out with custom-made water-cooled pyrometer probes containing a 90° deviation mirror at the end of the probe. The sighting tube of the probe is purged with nitrogen during the operation of the gas turbine to reduce contamination of the mirror surface. The probe contains Land TBTMS-R7QB thermometers with a silicon detector operating at 1μm wavelength. The probe is mounted in a probe traversing unit with two degrees of freedom (axial and circumferential, with respect to the probe axis). The traversing devices are bolted to flanges welded to the turbine casing. The probes penetrate the casing and the vane carrier radially (with respect to the machine). The dynamic seal between the cooling air and the ambient is provided by packings in the traversing device. The static seal between the hot gases and the cooling air is provided by metal bellows. Figure 7 shows a typical arrangement of the described components (in the sketch the arrangement is shown for a installation in the third stage). The pyrometer system is calibrated before and after each measurement cycle reducing the system uncertainty down to ±5 K.

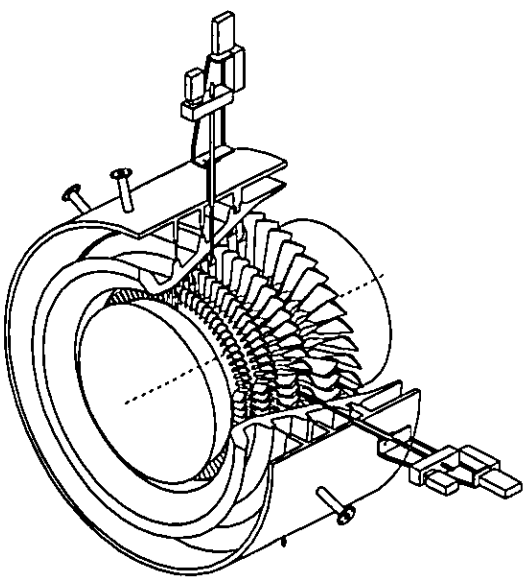

Fig. 7: Principle of gas turbine pyrometer measurements

Measurement of blade and vane temperatures

During measurements of vane temperatures from a pyrometer positioned upstream, the blockage of the flow channel by the probe alters the heat transfer and consequently the temperature distribution on the surface of the vane. Therefore, the surface temperature of the vanes cannot be determined under steady-state conditions. Changes in surface temperature do not occur spontaneously with the insertion of the probe. The thermal time constant is approx. 1 second for the measurements of interest. With the present technique, the probes are inserted as far as the full depth of the channel in 1/3 of the time constant. During this insertion, the position and the temperature signal are acquired simultaneously. After the near-hub position is reached, the probe is withdrawn quickly and rotated to a new view-angle. After a waiting period of approx. 4 time constants, the procedure is repeated for the new view angle. Thereby, the radial temperature is mapped for several view angles within the confines of the visible surface.

For such measurements, the probes are positioned just upstream of the leading edge of a vane and downstream of the trailing edge of a different vane. From here, the pyrometers map the temperatures on the surfaces of adjacent vanes. Figure 8 and Fig. 9 show the thermal map of the suction side of the first stage vane and the pressure side respectively.

Figure 10 and Fig. 11 show typical thermal maps of the suction and pressure side of the first stage rotor blade. For the measurement of blade temperatures, the obstruction of the flow channel by the probe is not relevant. The jagged pattern is due to the interpolation of only five radial measurement sections available for the first blade.

Measurement of radial temperature distributions

To compare the predicted gas temperatures to the actual profiles in the turbine, the radial temperature distributions were measured with a thermocouple in various cross-sections including the inlet of the first vane. These measurements were also carried out to provide boundary conditions for the design of the cooling system of blades and vanes. For these measurements the location and traversing device of the pyrometer was used. A typical radial temperature profile upstream of the second stage is shown in Fig. 12. Additional information on this measurements are given in Boehm et al. (1996).

Fig. 8 Temperature distribution of first vane suction side

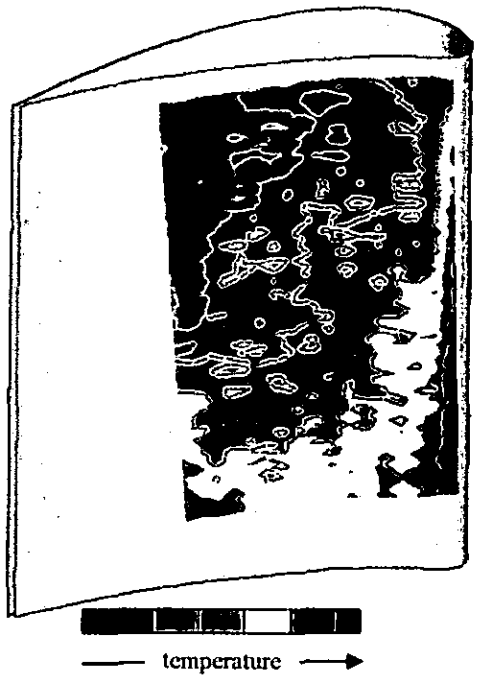

Fig. 9 Temperature distribution of first vane pressure side

Fig. 10 Temperature distribution of first blade suction side

Fig. 11 Temperature distribution of first blade pressure side

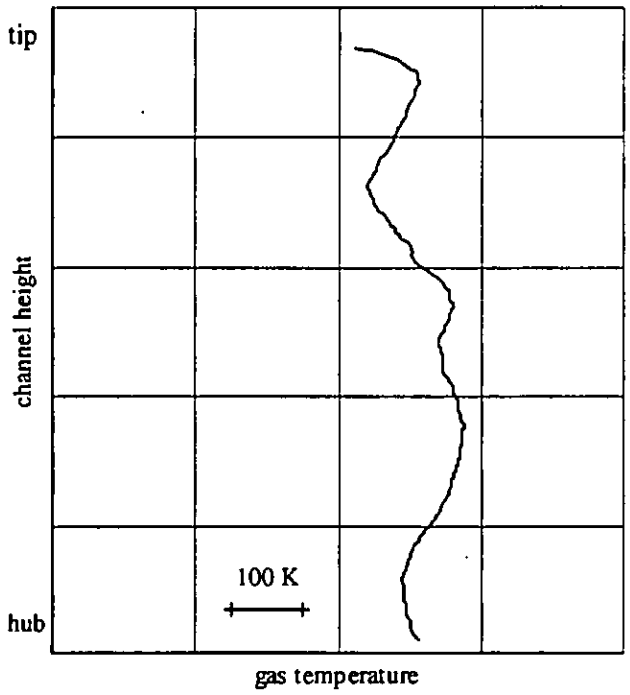

Fig. 12 Radial temperature profile

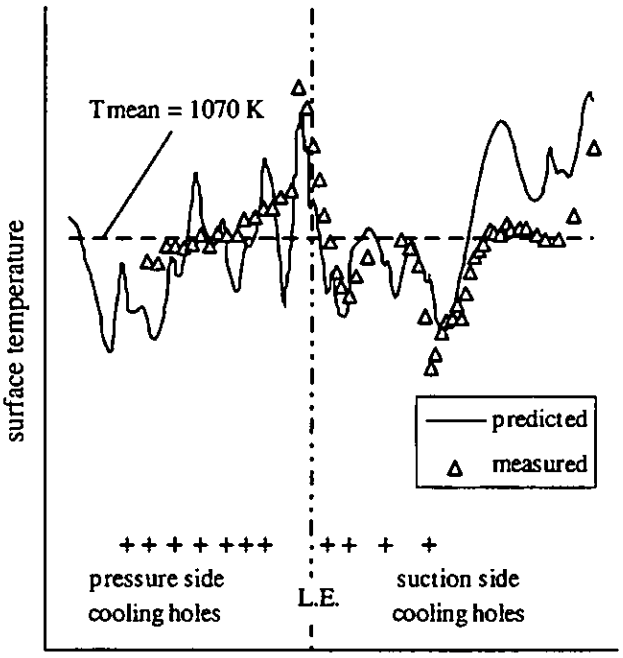

Fig. 13 Temperature profile of first vane

COMPARISON OF RESULTS

The comparison of the external surface temperature measurements with the predictions shows a good agreement, see Fig. 13 for the first stage vane and Fig. 14 for the blade. Hot gas and cooling air temperatures for the thermal analysis were taken from the measurements. The characteristics of the measured temperature distribution at mean section is well reproduced by the predictions for the vane and the blade. This is an indication that the system of external heat transfer, film cooling effectiveness and internal heat transfer is correctly simulated. However, if differences between predictions and measurements occur it is very difficult to trace them back, because manufacturing tolerances have to be added to the thermal design procedure. Because of the strong thermal loading, wall thickness deviations of only 0.1 mm may result in a temperature difference of 10 K. In general, due to the limited spatial resulution of the pyrometer the experimental results are smoothed out. Therefore, small peaks of the predictions are not reflected by the measurement.

At the trailing edge wall thicknes deviations in connection with the difficulty to predict effective gas temperatures can easily result in the shown temperature differences. The temperature deviations at the leading edge of the first blade are mainly due to the well known problem of accounting for the influence of strong wakes in combination with shower head film cooling acting on the thermal boundary layer of a rotating blade.

In general, predictions turned out to be conservative, such that measured temperatures are less than or equal to the predicted ones.

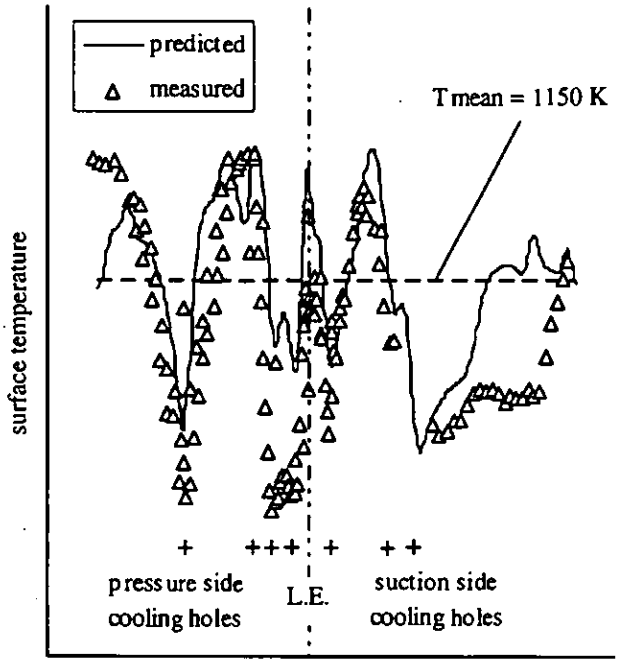

Fig. 14 Temperature profile of first blade

CONCLUSIONS

The aero-thermal design of the first turbine stage of the "3A-Series" gas turbine and results of the test run at the Berlin test facility have been presented.

State of the art CFD codes are used to calculate the two and three dimensional flow including the aerodynamic effect of the full coverage film cooling. The cooling system of the highly loaded airfoils include impingement, forced convection and film cooling devices. Boundary layer codes and a one dimensional network system are used to calculate the internal and external heat transfer. The comparison of measured and predicted surface temperature shows a good agreement. As the design temperature was never exceeded, the aero-thermal design of all turbine airfoils could be confirmed.

REFERENCES

Atkinson, W.H., and Guernard, R.N., 1978, "Turbine Pyrometry in Aircraft Engines," Paper No. 33/3. IEEE Electronic Show and Convention "Electro '78", Boston, USA.

Barber, R., 1969, "A Radiation Pyrometer Designed for In-Flight Measurement of Turbine Blade Temperatures," SAE Paper No. 690432.

Becker, B., Schulenberg, T., and Termuehlen, H., 1995, "The '3A-Series' Gas Turbines with HBR Combustors," ASME Paper 95-GT-458.

Benyon, T.G.R., 1981, "Turbine Pyrometrie — An Equipment Manufacturer's View," ASME Paper No. 81-GT-136.

Boehm, W., Raake, D., Regnery, D., Seume, J. and Terjung, K., 1996, "Testing the Model V84.3A Gas Turbine - Experimental Techniques and Results," ASME Paper 96-TA-14

Casey, M. V., 1994, "The Industrial Use of CFD in the Design of Turbomachinery," Proceedings, AGARD Lecture Series 195, Turbomachinery Design Using CFD, Ohio, United Staates, Ankara, Turkey, Munich, Germany, pp. 6-1 - 6-24.

De Lucia, M., and Lanfranchi, C., 1992, "An Infrared Pyrometry System for Monitoring Gas Turbine Blades: Development of a Computer Model and Experimental results" ASME Paper No. 92-GT-80.

De Lucia, M., and Masotti, G. 1995, "A Scanning Radiation Technique for Determining Temperature Distribution in Gas Turbines" Journal of Engineering for Gas Turbines and Power, Vol. 117, pp. 341-346.

Douglas, J., 1980, "High Speed Turbine Blade Pyrometry in Extreme Emviroments," in "Measurements Methods in Rotating Components of Turbomaschinery, pp. 335-343.

Janssen, M., Zimmermann, H., Kopper, F., and Richardson, J. 1995, "Application of Aero-engine Technology to Heavy Duty Gas Turbines," ASME Paper No. 95-GT-133.

Kato, M., and Launder, B.E., 1993, "The Modelling of Turbulent Flows around Stationary and Vibrating Cylinders," Proceedings, Ninth Symposium on Turbulent Shear Flows, Kyoto, Japan, pp. 10.4.1 - 10.4.6.

Kruse, H., 1985, "Effects of Hole Geometry, Wall Curvature and Pressure Gradient on Film Cooling Downstream of a Single Row," Proceedings, AGARD-CP-390, Heat Transfer and Cooling in Gas Turbines, Bergen, Norway, pp. 8-1 - 8-13.

Launder, B. E., and Spalding, D. B., 1974, "The Numerical Computation of Turbulent Flows," Comp. Meth. Appl. Mech. Eng., Vol. 3, pp. 269 - 289.

L'Ecuyer, M. R., and Soechting, F. O., 1985, "A Modell for Correlating Flat Plate Film Cooling Effectiveness for Rows of Round Holes," Proceedings, AGARD-CP-390, Heat Transfer and Cooling in Gas Turbines, Bergen, Norway, pp. 19-1 - 19-12.

Moon, H.K., Glezer, B., Mink, B., and Marvin, W., 1995, "Development of Wide Range Temperature Pyrometer for Gas Turbine Application," ASME Paper No. 95-GT-126.

Reichert, A. W., and Janssen, M., 1996, "Cooling and Sealing Air System in Industrial Gas Turbine Engines," ASME Paper 96-GT-256.

Rohy, D.A., and Compton, W.A. 1973, "Radiation Pyrometer for Gas Turbine Blades," Final Report for Contract NAS8 28953.

Schenk, B., Pucher, H., Neuer, G., Schreiber, E., and Brandt, R. 1994, "Einsatz der berührungslosen Temperaturmeßtechnik zur Bestimmung der Oberflächentemperaturverteilung von keramischen Rotorbauteilen im Betrieb," in "Thermische Strömungsmaschinen: Fortschritte in der Strömungsmaschinentechnik," VDI Verlag, Düsseldorf, VDI Berichte Nr. 1109, pp. 293-315.

Schenk, B. and Raake, D., 1996, "Fast Response Turbine Pyrometry for High Temperature Gas Turbine Applications - Present State of Technology and Future Demands," HTMTC and BAM Symposium "Local Strain and Temperature Measurements in non-uniform Fields at elevated Temperatures," March 14-15, 1996, Berlin, Germany.

Scheuerer, G., 1983, "Entwicklung eines Verfahrens zur Berechnung zweidimensionaler Grenzschichten an Gasturbinenschaufeln," Ph.D. Thesis, University of Karlsruhe, Germany.

Schoenung, B., and Rodi, W., 1987, "Prediction of Film Cooling by a row of Holes With a Two-Dimensional Boundary Layer Procedure," Journal of Turbomachinery, Vol. 109, pp. 579 - 587.

Schulenberg, T., and Bals, H., 1987, "Blade Temperature Measurements of Model V84.2 100 MW/60 Hz Gasturbine," ASME Paper No. 87-GT-135.

Schulenberg, T., and Zimmermann, H., 1995, "New Blade Design of Siemens Gas Turbines," Proceedings, POWER-GEN EUROPE '95, Amsterdam, The Netherlands, Vol. 5, pp. 639 - 661.

Sellers, R.R., Przirembel, H.R., Clevenger, D.H., and Lang, J.L., 1989, "The Use of Optical Pyrometers in Axial Flow Turbines," AIAA Paper No. 89-2692.